Adenosine signaling and its downstream target mod(mdg4) modify the pathogenic effects of polyglutamine in a *Drosophila* model of Huntington's disease

Yu-Hsien Lin[1,2*], Houda Ouns Maaroufi[1,2], Lucie Kucerova[1], Lenka Rouhova[1,2], Tomas Filip[1,2], Michal Zurovec[1,2*]

[1]Biology Centre of the Czech Academy of Sciences, Institute of Entomology, Ceske Budejovice, Czech Republic, [2]Faculty of Science, University of South Bohemia, Ceske Budejovice, Czech Republic

*Correspondence and requests for materials should be addressed to Y.H.L. (email: r99632012@gmail.com) and M.Z. (email: zurovec@entu.cas.cz).

Abstract

Dysregulation of adenosine (Ado) homeostasis has been observed in both rodent models and human patients of Huntington's disease (HD). However, the underlying mechanisms of Ado signaling in HD pathogenesis are still unclear. In the present study, we used a *Drosophila* HD model to examine the concentration of extracellular Ado (e-Ado) as well as the transcription of genes involved in Ado homeostasis and found similar alterations. Through candidate RNAi screening, we demonstrated that silencing the expression of adenosine receptor (*adoR*) and equilibrative nucleoside transporter 2 (*ent2*) not only significantly increases the survival of HD flies but also suppresses both retinal pigment cell degeneration and the formation of mutant Huntingtin (mHTT) aggregates in the brain. We compared the transcription profiles of *adoR* and *ent2* mutants by microarray analysis and identified a downstream target of AdoR signaling, *mod(mdg4)*, which mediates the effects of AdoR on HD pathology in *Drosophila*. Our findings have important implications for the crosstalk between Ado signaling and the pathogenic effects of HD, as well as other human diseases associated with polyglutamine aggregation.

Introduction

Adenosine (Ado) is one of the most common neuromodulators in the nervous system of vertebrates as well as invertebrates and modulates synaptic transmission[1,2]. Under normal conditions, the extracellular Ado (e-Ado) concentration is in the nanomolar range, which is sufficient to modulate the appropriate adenosine receptors (AdoRs) in the brain cells tonically[3]. However, under pathological circumstances the e-Ado level may increase up to 100-fold. In these conditions, Ado functions as an imperfect neuroprotector; in some cases it may be beneficial and in others may worsen tissue damage[4]. Recent experiments with knockout mice for all four *adoRs* demonstrated that Ado signaling is less involved in baseline physiology and likely more crucial for its roles as a signal of stress, damage, and/or danger[5]. It has also been suggested that Ado signaling is mainly engaged when an allostatic response is needed[6].

Due to its impact on important physiological functions in the brain, e-Ado signaling has attracted attention as a possible therapeutic agent in Huntington's disease (HD)[7], a dominant hereditary neurodegenerative disorder caused by a mutation in the Huntingtin gene (*htt*). Mutated HTT protein (mHTT) contains an expanded polyglutamine (polyQ) tract encoded by 40 to more than 150 repeats of CAG trinucleotide[8]. Although mHTT is ubiquitously expressed in the central nervous system (CNS) and peripheral cells in HD patients, it predominantly affects striatal neurons that contain a higher density of adenosine receptors A2A ($A_{2A}R$) and A1 (A_1R)[9]. Several studies have demonstrated that the abnormality of AdoRs activity, especially $A_{2A}R$ in the striatum, contributes to HD pathogenesis[10,11]. In addition, the alteration of adenosine tone and the upregulation of striatal equilibrative nucleoside transporters (ENTs), facilitating Ado transport across the cytoplasmic membrane, suggest that e-Ado concentration could serve as a HD biomarker for assessing the initial stages of neurodegeneration[12,13]. However, the complexity of the system modulating Ado metabolism and the crosstalk between individual AdoRs, as well as their interactions with purinergic (P2) or dopamine receptors, impedes the characterization of HD pathophysiology and downstream mechanisms of e-Ado signaling [14,15].

Drosophila expressing human mHTT has previously been demonstrated as a suitable model system for studying gene interactions in polyQ pathology, and has been used to elicit a number of modifiers for symptoms of HD [16,17]. *Drosophila* e-Ado signaling is a relatively simple system compared to mammals; it contains a single AdoR isoform (cAMP simulation) and lacks P2X receptors [18,19]. Human homologs of the *Drosophila* genes involved in the regulation of Ado homeostasis and AdoR are shown in Fig. S1. The lack of adenosine deaminase 1 (ADA1) in *Drosophila* indicates that adenosine deaminase-related growth factors (ADGFs, related to ADA2), together with adenosine kinase (AdenoK), are the major metabolic enzymes converting extra- and intra-cellular adenosine to inosine and AMP, respectively [20-22]. e-Ado signaling in *Drosophila* is involved in regulating various physiological and pathological processes, including modulation of synaptic plasticity, JNK-mediated stress response, hematopoiesis, and metabolic switching upon immune challenges [23-25].

In the present study, we performed a candidate RNAi screen examining the role of Ado signaling in a *Drosophila* HD model. We co-expressed exon 1 with a polyglutamine tract of normal human *htt* Q20 or pathogenic *mhtt* Q93[17] together with *UAS-RNAi* or *UAS*-overexpression constructs specific for *adoR*, Ado transporters, and Ado metabolic enzymes in *Drosophila*. We demonstrated that the downregulation of *adoR* and *ent2* expression reduces cell death, mortality and the formation of mHTT aggregates. In addition, we identified a number of differentially-expressed genes in response to Ado signaling and showed that *mod(mdg4)* is a downstream target of AdoR that mediates its effect in HD pathogenesis.

Results

Phenotypes of *Drosophila* expressing mHTT

To verify the effect of mHTT expression on *D. melanogaster*, we used a *UAS/GAL4* system for targeted gene expression. Flies overexpressing normal exon 1 from human huntingtin (Q20 HTT), or its mutant pathogenic form (Q93 mHTT), were driven by the pan-neuronal driver, *elav-GAL4*. The results showed that expression of mHTT under the *elav-GAL4*

driver in the *Drosophila* brain is not lethal during the larval stage (Fig. S2A) but reduces both the adult eclosion rate (Fig. S2B) and adult lifespan (Fig. S2C). These results are consistent with previous observations[26].

Disturbance of extracellular adenosine (e-Ado) homeostasis in HD larvae

A recent study of human HD patients reported a reduced concentration of e-Ado in the cerebrospinal fluid [27]. To determine whether e-Ado levels are also altered in HD *Drosophila*, we compared e-Ado levels in the hemolymph of last-instar larvae ubiquitously expressing Q20 HTT and Q93 mHTT driven by the *daughterless-Gal4* driver (*da-GAL4*). The results showed that the e-Ado concentration in the hemolymph of Q93-expressing larvae was significantly lower compared to larvae expressing Q20 or control *da-GAL4* (Fig. 1A).

Since e-Ado concentration may be associated with the level of extracellular ATP (e-ATP), we also examined its titer in the hemolymph of larvae with the same genotypes as the above experiment. As shown in Fig. 1B, there was no significant difference in e-ATP levels between Q20, Q93, and control *da-GAL4* larvae. We thus postulated that the lower level of e-Ado in Q93 larvae might be affected by changes in proteins involved in Ado metabolism or transportation.

Altered transcriptions of genes involved in Ado homeostasis in HD *Drosophila*

Earlier reports have shown that the expression of several genes involved in Ado homeostasis, including Ado receptor, transporters, and genes involved in Ado metabolism, are abnormal in human HD patients as well as in HD mice [28-30]. Since homologous proteins have also been shown to control Ado homeostasis in flies (Fig. S1), we compared the expression of three *Drosophila adgf* genes (*adgf-a*, *adgf-c*, *adgf-d*), adenosine kinase (*adenoK*), adenosine transporters (*ent1*, *ent2*, *ent3*, *cnt2*), and adenosine receptor (*adoR*) in the brains of Q93- and Q20-expressing larvae. The results showed that the expression of *adgf-a* and *adgf-d*, as well as transporters *ent1*, *ent2*, and *ent3* in the brain of Q93 larvae were significantly lower than in Q20 larvae (Fig. 1D). The expression of *cnt2* and *adoR* showed no difference between Q93 and Q20 larvae.

In order to assess progressive changes in transcription profiles associated with HD pathogenesis, we further examined the expression of genes involved in Ado homeostasis in the heads of 5- and 15-day-old adults, roughly corresponding to early- and late-stage HD (Fig. S2C). Unlike in the larval stage, the expression of metabolic genes *adgf-c*, *adgf-d*, and *adenoK*, and transporter *ent1*, in five-day-old adults was found to be higher in Q93 flies than Q20 flies (Fig. 1E). In addition, 15-day-old Q93 flies showed higher expression of *adgf-d* and *adenoK* (Fig. 1F). Previous studies in *Drosophila* have shown that the downregulation of the transporter *ents* decreases e-Ado concentration [23,24]; hence, the reduced expression of three *ent* genes could explain why the e-Ado level is lower in Q93 larvae. Moreover, it has also been shown that the expression of *adgfs* as well as *adenoK* follows the levels of e-Ado upon stress conditions [31,32], suggesting that the lower expression of *adgfs* in Q93 larvae and the higher expression in Q93 adults might be a consequence of elevated e-Ado concentrations resulting from HD pathogenesis.

Functional characterization of Ado homeostasis and signaling in HD flies

To understand the effects of alterations in Ado homeostasis on polyQ pathology, we used the pan-neuronal driver, *elav-GAL4*, for RNAi-mediated silencing of the genes involved in Ado transport, metabolism, and *adoR* in Q93-expressing flies and assessed their survival and formation of mHTT aggregates. In addition, we also co-expressed Q93 with RNAi transgenes in the eyes by using the *gmr-GAL4*[33,34] driver and compared levels of retinal pigment cell degeneration.

Silencing the transcriptions of Ado metabolic enzymes showed that only the RNAi of *adgf-D* increased the number of eclosion rate (Fig. 2A). Silencing *adgf-A* and *adenoK*, but not *adgf-D* or *adgf-C* RNAi, extended the adult lifespan of Q93-expressing flies (Fig. 2B). To ensure that the mortality of the HD flies was mainly caused by Q93 expression and not by RNAi constructs, we recorded the survival of flies co-expressing normal *htt* Q20 together with RNAi transgenes until all corresponding experimental flies (expressing Q93 together with RNAi constructs) died (Fig. S3A). However, silencing *adgfs* or *adenoK* only affected survival and did not significantly influence mHTT aggregation (Fig. 2C&D) or retinal pigment cell degeneration (Fig. 2E).

Next, we examined the RNAi silencing of *adoR* and Ado transporters in Q93 and control Q20 flies. The results showed that knocking down the expression of *adoR* as well as two transporters, *ent1* and *ent2*, significantly increased the eclosion rate (Fig. 3A) and adult lifespan (Fig. 3B). The RNAi silencing of *ent2* and *adoR* extended the lifespan of HD flies to 30 and 40 days, respectively, which is about 1.5~2 times longer than that of HD flies. In contrast, knocking down *cnt2* expression did not change the viability of HD flies, and knocking down *ent3* did not influence the eclosion rate, although it increased mortality and shortened the lifespan of adult HD flies. The survival of control flies expressing Q20 with individual RNAi constructs are shown in Fig. S3B. mHTT aggregation was significantly reduced (to 50%) in *adoR* RNAi flies (Fig. 3C&D), and a similar suppression of mHTT aggregate formation was also observed in 20-day-old HD flies (Fig. S4). An examination of eye phenotypes in *ent2* RNAi flies showed a significant reduction in retinal pigment cell death (Fig. 3E), but surprisingly we did not observe a significant rescue of cell death by silencing *adoR* (Fig S5). We therefore postulated that it might be due to insufficient RNAi efficiency for suppressing AdoR signaling in the eye. To test this, we combined Q93 flies with the *adoR* RNAi transgene under a *adoR* heterozygote mutant background ($AdoR^1$/+) or with $AdoR^1$ homozygote mutant, and both showed significantly decreased retinal pigment cell degeneration similar to *ent2*–RNAi flies (Fig. 3E).

To further validate the RNAi results, we studied flies simultaneously expressing Q93 and overexpressing *ent2*, *adoR*, *adgf-A*, and *adenoK* in the brain and assessed the adult lifespans. Since silencing these genes extended the lifespan of HD flies (Figs. 2B&3B), we expected the opposite effect upon overexpression. As shown in Fig. S6A, *ent2* overexpression significantly increased the mortality of early-stage HD flies; the survival of 5-day-old flies dropped to 60% for HD flies in contrast to 90% for Q93 control flies, and the lifespan of HD flies was significantly shorter than control flies expressing either Q93 alone or together with *gfp* RNAi. Consistently, we co-expressed strong and weak *adoR* overexpressing transgenes with Q93 and both significantly increased the mortality and shortened the lifespan of Q93 flies. The effects of shortening the lifespan were more severe than with *ent2* overexpression. Nevertheless, the increase in mortality by *adgf-A* and *adenoK* overexpression was not as strong as that caused by *ent2* and *adoR* overexpression, although both still showed a significant difference to either Q93 control or Q93/*gfp* RNAi

control by weighted log-rank test (Fig. S6B). Hence, we concluded that overexpressing the examined genes enhances the effect of mHTT, resulting in the increased mortality of HD flies. Our results demonstrate that the overexpression and silencing of *ent2* or *adoR* has a stronger influence over HD pathology than genes involved in Ado metabolism.

Interactions of AdoR with ENT1 and ENT2

In order to investigate whether there is a synergy between the effects of AdoR and ENTs, we co-expressed *adoR* RNAi constructs with *ent1* RNAi or *ent2* RNAi in Q93-expressing flies. As shown in Fig. 4A, the silencing of both *ent2* and *adoR* has the same effect as silencing only *adoR*, indicating that ENT2 and AdoR are in the same pathway. Interestingly, the double knockdown of *ent1* and *adoR* shows a sum of individual effects on lifespan which is longer than the knockdown of *adoR* alone. There seems to be a synergy between ENT1 and AdoR suggesting that ENT1 may have its own effect, which is partially independent from AdoR signaling.

Next, we investigated our hypothesis that the source of e-Ado, which contributes to AdoR activation in Q93 flies, is mainly intracellular and released out of the cells by ENTs. We conducted an epistasis analysis by combining mHTT with *adoR* overexpression and *ent1* or *ent2* RNAi. The results showed that *adoR* overexpression increased the mortality of Q93 flies while the combination of *adoR* overexpression with either *ent1* or *ent2* RNAi minimized the increased mortality caused by *adoR* overexpression (Fig. 4B). Notably, Q93 flies expressing *ent2* RNAi and overexpressing *adoR* had the longest lifespan in comparison to Q93 control or *ent1* RNAi flies. These results suggest that AdoR signaling needs functional Ado transportation to carry out its effect and thus the Ado efflux from these cells is needed for AdoR activity (Fig. 4C&D). The source of e-Ado, which contributes to AdoR activation causing HD pathogenesis, seems to be intracellular and it is mainly released out of the cells through ENT2.

AMPK is not involved in *Drosophila* HD pathogenesis

AMP-activated protein kinase (AMPK) is one of the key enzymes maintaining energy balance within a cell by adjusting anabolic and catabolic pathways [35]; both Ado receptors and transporters have been implicated in its activation [36-39]. Activation of AMPK is

206 beneficial at early stages in mammalian HD models [40]; however, in the late stage of the
207 disease it may worsen neuropathological and behavioral phenotypes [41].

208 To find out whether the above-described effects of e-Ado signaling and transport on HD
209 flies are mediated by AMPK, we co-expressed *Q93 mHTT* with three different recombinant
210 forms of AMPK α subunit[42,43], including wild-type AMPKα [M], a phosphomimetic-
211 activated form of AMPKα [T184D], and dominant negative AMPK [DN], and assessed the
212 survival of HD flies. The results showed that neither the activation nor the inhibition of
213 AMPK signaling influenced the eclosion rate (Fig. S7A) or lifespan (Fig. S7B).

214 To further confirm the genetic data related to AMPK activation or inhibition, we
215 pharmaceutically inhibited AMPK signaling by feeding the larvae with AMPK inhibitor,
216 dorsomorphin (Compound C) [44]. The results showed that although dorsomorphin had an
217 effect on the development of larvae expressing normal Q20 HTT, it did not influence the
218 eclosion of Q93-expressing larvae (Fig. S7C). Overall, our results show that, unlike in
219 mammalian HD models, AMPK signaling does not play a significant role in the
220 pathological manifestations of mHTT in *Drosophila*.

221 **Identification of potential downstream targets of the AdoR/ENT2 pathway by**
222 **microarray analysis**

223 Our above results indicate that ENT2 and AdoR contribute to mHTT pathogenesis in HD
224 *Drosophila* and work in the same pathway. To identify their downstream target genes, we
225 compared the expression profiles of larvae carrying mutations in *adoR* or *ent2* as well as
226 adult *adoR* mutants using microarrays (Affymetrix), shown as a Venn diagram in Fig. 5A
227 and B. The intersection between each mutant contains differentially expressed transcripts
228 in all three data sets, including six upregulated (Fig. 6A) and seven downregulated mRNAs
229 (Fig. 5B). Interestingly, according to Flybase (http://flybase.org), four of these genes were
230 expressed in the nervous system (*ptp99A* was upregulated, while *CG6184*, *cindr*, and
231 *mod(mdg4)* were downregulated) (Fig. 5C).

232 To validate the microarray data, we knocked down *adoR* expression in the brain and
233 examined the transcription of the four candidate genes expressed in the nervous system by
234 qPCR. The results revealed that *ptp99A* and *mod(mdg4)* had the same expression trends as

observed in the microarrays (Fig. 5D). We further examined whether the expression of *ptp99A* and *mod(mdg4)* are influenced by an increase of e-Ado level. As shown in Fig. 6E, Ado microinjection significantly increased *mod(mdg4)* expression and decreased *ptp99A* expression, confirming that *mod(mdg4)* is positively regulated and *ptp99A* is negatively regulated by the AdoR/ENT2 pathway.

Suppression of *mod(mdg4)* decreased mHTT aggregation and increased survival of HD flies

In order to examine the potential roles of *ptp99A*, *CG6184*, *cindr*, and *mod(mdg4)* genes in HD pathogenesis, we used RNAi to silence them in HD flies. The results showed that only the RNAi silencing of *mod(mdg4)* extended their lifespan. As shown in Figure 6A, the survival curve of HD flies with a silenced *mod(mdg4)* gene was almost identical to the curve specific for *adoR* RNAi HD flies; this effect was stronger than in *ent2* RNAi HD flies. In addition, *mod(mdg4)* RNAi significantly decreased the formation of mHTT inclusions (Fig. 6B&C) and suppressed retinal pigment cell degeneration (Fig. 7D). In contrast to *mod(mdg4)*, RNAi silencing of the other three genes did not show any significant effect.

To further confirm that *mod(mdg4)* is downstream target of the AdoR pathway and regulated by e-Ado signaling, we first checked the expression of *mod(mdg4)* in larval brains and adult heads of HD flies using qPCR. In Q93 larvae, we found that both the expression level of *mod(mdg4)* (Fig. 7A) and the e-Ado level was lower than in Q20-expressing controls (Fig. 1A). For the 15-day-old (roughly corresponding to late-stage HD) Q93 adults, there was no difference in *mod(mdg4)* expression compared to Q20 control adults (Fig. 7A). We next examined the epistasis relationship between *ent2*, *adoR*, and *mod(mdg4)* by combining overexpression of *ent2* or *adoR* *mod(mdg4)* RNAi in Q93-expressing flies. The results showed that *mod(mdg4)* RNAi suppressed the lethal effects caused by the overexpression of *ent2* and *adoR* (Fig. 8B). These results indicate that *mod(mdg4)* serves as a downstream target of AdoR signaling involved in the process of mHTT inclusion formation and other pathogenic effects (Fig. 7C).

The *mod(mdg4)* locus of *Drosophila* contains several transcription units encoded on both DNA strands producing 31 splicing isoforms[45]. As shown in Fig. 5B, two of the

mod(mdg4)-specific microarray probes which target 11 *mod(mdg4)* splicing isoforms (Tab. S2) were downregulated in all three datasets. We performed splice form-specific qPCR analysis and found that *adoR* RNAi silencing leads to the downregulation of multiple *mod(mdg4)* isoforms (Fig. 7D), suggesting that AdoR signaling regulates multiple isoforms.

Discussion

Considerable dysregulation of Ado homeostasis has been observed in HD human patients and mice, but the mechanisms of such changes related to HD pathogenesis still need to be characterized[46]. The present study examined the e-Ado titer in the hemolymph of HD *Drosophila* larvae and found that it is lower in Q93-expressing larvae (Fig. 1). Although we did not measure the e-Ado titer in adult flies (due to a problem in acquiring a sufficient amount of hemolymph), the dynamic changes in expression levels of genes involved in Ado homeostasis (Fig. 1D-E), as well as the AdoR-regulated gene, *mod(mdg4)* (Fig. 8A), indicated that e-Ado titer and AdoR activity are variable in different stages of HD. Such dynamic changes of e-Ado homeostasis have also been observed in rodent HD models, whereby striatal adenosine tone is lower during the early stage of the disease and increased during the later stages[13,47].

Both the activation and inhibition of $A_{2A}R$ by pharmacological treatments have shown benefits in mammalian HD models. In R6/2 mice, the beneficial effect of activating $A_{2A}R$ is thought to occur *via* the inhibition of AMPK nuclear translocation (which contributes to HD pathogenesis including brain atrophy, neuron death, and increased mHTT aggregates formation) [41]. Beneficial effects by antagonizing $A_{2A}R$ with SCH58261 in R6/2 mice include reduced striatal glutamate and adenosine outflow as well as restoring emotional behavior and susceptibility to NMDA toxicity [47,48]. A_1R activation has also been shown to have neuroprotective effects; however, the chronic administration of A_1R agonists (leading to a desensitisation of A1 receptors) increases neuronal loss whereas the chronic administration of A_1R antagonists (inducing an upregulation of A1 receptors) improves survival and neuronal preservation in the same model [49]. Our results show that the genetic depletion of AdoR has beneficial effects on HD flies, while the activation of AdoR contributes to mHTT pathogenesis and aggregates formation.

We observed a non-additive interaction between AdoR and ENT2 characteristic for epistasis relationship (Fig. 4B), indicating that ENT2 is required for the transportation of Ado from the intra- to extracellular environment which activates AdoR and, in turn, enhances the effects of mHTT. Our previous report showed that both ENT2 and AdoR participate in modulating synaptic transmission, and that both *adoR* and *ent2* mutations cause defects in associative learning in *Drosophila*[25]. Consistently, both the inhibition of Ado release by the knockdown of *ent2* in hemocytes and the mutation of *adoR* suppress metabolic reprogramming and hemocyte differentiation upon immune challenges[23]. Furthermore, another report showed that the disruption of epithelial integrity by Scribbled (*Scrib*) RNAi stimulates Ado release through ENT2, subsequently activating AdoR that, in turn, upregulates tumor necrosis factor (TNF) production which activates JNK signaling[24]. Interestingly, while the effects of *ent2* and *adoR* RNAi in HD flies were found to completely overlap, *ent1* RNAi showed a synergistic effect, suggesting potential AdoR-independent mechanisms (Fig. 4A). These results correspond to our previous report showing that *Drosophila* ENT1 has lower specificity for Ado transportation in comparison to ENT2[50]. The altered expression of *ent1*, as well as the RNAi effect in HD flies, might be associated with the disturbance of nucleotide homeostasis, similar to that observed in R6/2 and Hdh^{Q150} mice[51].

We identified a downstream target of the AdoR pathway, mod(mdg4), which contributes to the effects of mHTT in the *Drosophila* HD model. The *mod(mdg4)* gene has previously been implicated in the regulation of position effect variegation, chromatin structure, and neurodevelopment[52]. The altered expression of *mod(mdg4)* has also been observed in flies expressing untranslated RNA containing CAG and CUG repeats[53,54]. In addition, *mod(mdg4)* has complex splicing, including *trans*-splicing, producing at least 31 isoforms[55]. All isoforms contain a common N-terminal BTB/POZ domain which mediates the formation of homomeric, heteromeric, and oligomeric protein complexes[56-58]. Among these isoforms, only two [including *mod(mdg4)*-56.3 (isoform H) and *mod(mdg4)*-67.2 (isoform T)] have been functionally characterized. *Mod(mdg4)*-56.3 is required during meiosis for maintaining the chromosome pairing and segregation in males[59,60]. Mod(mdg4)-67.2 interacts with Suppressor of hairy wing [Su(Hw)] and Centrosomal protein 190 kD (CP190) forming a chromatin insulator complex which inhibits the action

of the enhancer on the promoter, and is important for early embryo development and oogenesis[61-63]. Although our results showed that silencing all *mod(mdg4)* isoforms decreases the effects of mHTT (Fig. 6), we could not clarify which of the isoforms is specifically involved in HD pathogenesis because AdoR signaling regulates multiple isoforms (Fig. 7D). Interestingly, an earlier report on protein two-hybrid screening indicated that Mod(mdg4) interacts with six Hsp70 family proteins[64,65], and Hsp70 proteins are known for their contribution to the suppression of polyQ aggregates formation and neurodegeneration [66,67]. Further study will be needed to identify the specific *mod(mdg4)* isoform involved in HD pathogenesis, and whether a decrease in mHTT aggregates by mod(mdg4) RNAi is connected to Hsp70 interaction.

In summary, we observed an alteration in the e-Ado concentration and expression of genes involved in Ado homeostasis in a *Drosophila* HD model. By candidate RNAi screening, we demonstrated that the silencing of *ent2* and *adoR* increases the survival of HD flies in addition to suppressing retinal cell degeneration and mHTT aggregate formation. We also showed that the activation of e-Ado signaling enhances the effects of mHTT. Furthermore, we found that *mod(mdg4)* is a downstream target of the AdoR pathway and plays a major role in the pathogenesis of HD flies. Our work enhances our understanding of e-Ado signaling in HD pathogenesis and may open up new opportunities for HD pharmacological intervention.

Materials and methods

Fly stocks

Flies were reared at 25 ℃ on standard cornmeal medium. The following RNAi lines were acquired from the TRiP collection (Transgenic RNAi project) at Harvard Medical School: adgfA-Ri (BL67233), adgfC-Ri (BL42915), adgfD-Ri (BL56980), adenoK-Ri (BL64491), ent1-Ri (BL51055), adoR-Ri (BL27536), gfp-Ri (BL41552), mod(mdg4)-Ri (BL32995), cindr-Ri (BL38976), and ptp99A-Ri (BL57299). The following RNAi lines were acquired from the Vienna Drosophila RNAi Center (VDRC): ent2-Ri (ID100464), ent3-Ri (ID47536), cnt2-Ri (ID37161), and cg6184-Ri (ID107150). The following lines were

355 provided by the Bloomington Drosophila Stock Center: UAS-AMPKα^{T184D} (BL32110),
356 UAS-AMPKα^{M} (BL32108), UAS-AMPKα^{DN} (AMPKα^{K57A}, BL32112), and elav^{C155}-
357 GAL4 (BL458).
358 Flies overexpressing human normal huntingtin (HTT) exon 1, Q20Httexon^{1111F1L} or mutant
359 pathogenic fragments (mHTT), Q93Httexon^{14F132} were obtained from Prof. Lawrence
360 Marsh (UC Irvine, USA)[17]. The UAS-overexpression lines, Ox-adenoK and Ox-adoR (s),
361 were obtained from Dr. Ingrid Poernbacher (The Francis Crick Institute, UK)[24]. gmr-GAL4
362 was obtained from Dr. Marek Jindra (Biology Centre CAS, Czechia). da-GAL4 was
363 obtained from Dr. Ulrich Theopold (Stockholm University). The UAS overexpression
364 strains Ox-adgfA, Ox-ent2, and Ox-adoR (w), as well as adoR^{1} and ent2^{3} mutant flies, were
365 generated in our previous studies[25,68-70].
366

367 **Eclosion rate and adult lifespan assay**

368 For assessing the eclosion rate, male flies containing the desired RNAi or overexpression
369 transgene (RiOx) in the second chromosome with genotype w^{1118}/Y; RiOx /CyO; UAS-
370 Q93/MKRS were crossed with females of *elav-GAL4*; +/+; +/+. The ratio of eclosed adults
371 between *elav-GAL4*/+; RiOx/+; UAS-Q93/+ and *elav-GAL4*/+; RiOx/+; +/MKRS was then
372 calculated. If the desired RiOx transgene was in the third chromosome, female flies
373 containing *elav-GAL4*; +/+; RiOx were crossed with male w^{1118}/Y; +/+; UAS-Q93/MKRS,
374 and the ratio of eclosed adults between *elav-GAL4*; +/+; RiOx/UAS-Q93 and *elav-GAL4*;
375 +/+; RiOx/MKRS was calculated.
376 For the adult lifespan assay, up to 30 newly emerged female adults were placed in each
377 cornmeal vial and maintained at 25 ℃. At least 200 flies of each genotype were tested, and
378 the number of dead flies was counted every day. Flies co-expressing RiOx and Q20 were
379 used for evaluating the effect of RNAi or overexpression of the desired transgenes (Fig.
380 S3A&B).
381

382 **Extracellular adenosine and ATP level measurements**

383 To collect the hemolymph, six third instar larvae (96 hours post-oviposition) were torn in
384 150 µl of 1× PBS containing thiourea (0.1 mg/ml) to prevent melanization. The samples

were then centrifuged at 5000× *g* for 5 min to separate the hemocytes and the supernatant was collected for measuring the extracellular adenosine or ATP level. For measuring the adenosine titer, 10 µl of hemolymph was mixed with reagents of an adenosine assay kit (Biovision) following the manufacturer's instructions. The fluorescent intensity was then quantified (Ex/Em = 533/ 587 nm) using a microplate reader (BioTek Synergy 4). For measuring the ATP level, 10 µl of hemolymph was incubated with 50 µl of CellTiter-Glo reagent (Promega) for 10 min. Then, the luminescent intensity was quantified using an Orion II microplate luminometer (Berthold). To calibrate the standard curve of ATP concentration, 25 µM ATP standard solution (Epicentre) was used for preparing a concentration gradient (0, 2, 4, 6, 8, 10 µM) of ATP solution and the luminescent intensity was measured for each concentration. The protein concentration of the hemolymph sample was determined by A280 absorbance using a NanoDrop 2000 spectrophotometer (Thermo Fisher). The adenosine and ATP concentrations were first normalized to protein concentration. Then, the values of Q20 and Q93 samples were normalized to values of the *GAL4* control sample. Six independent replicates for each genotype were performed for the analysis of adenosine and ATP levels.

RNA extraction

The brains from 10 third-instar larvae (96 hours post-oviposition), heads from 30 female adults (5 days or 15 days old) or 15 whole female flies were collected. The samples were first homogenized in RiboZol (VWR) and the RNA phase was separated by chloroform. For brain or head samples, the RNA was precipitated by isopropanol, washed in 75% ethanol and dissolved in nuclease-free water. For whole fly samples, the RNA phase was purified using NucleoSpin RNA columns (Macherey-Nagel) following the manufacturer's instructions. All purified RNA samples were treated with DNase to prevent genomic DNA contamination. cDNA was synthesized from 2 µg of total RNA using a RevertAid H Minus First Strand cDNA Synthesis Kit (Thermo Fisher Scientific).

Adenosine injection

Three- to five-day-old female adults were injected with 50 nl of 10 mM adenosine using a NANOJECT II (Drummond Scientific); control flies were injected with 50 nl of 1× PBS. Two hours post-injection, 15 injected flies for each replicate were collected for RNA extraction.

Microarray analysis

The Affymetrix GeneChip® *Drosophila* genome 2.0 array system was used for microarray analysis following the standard protocol: 100 ng of RNA was amplified with a GeneChip 3′ express kit (Affymetrix), and 10 μg of labeled cRNA was hybridized to the chip according to the manufacturer's instructions. Statistical analysis of array data were described previously in our studies[71,72]. Storey's q value (false discovery rate, FDR) was used to select significantly differentially transcribed genes ($q < 0.05$). Transcription data are shown in Table S2.

qPCR and primers

5× HOT FIREPol® EvaGreen® qPCR Mix Plus with ROX (Solis Biodyne) and an Eco Real-Time PCR System (Illumina) were used for qPCR. Each reaction contained 4 μl of EvaGreen qPCR mix, 0.5 μl each of forward and reverse primers (10 μM), 5 μl of diluted cDNA and ddH2O to adjust the total volume to 20 μl. The list of primers is shown in Table S1. The expression level was calculated using the $2^{-\Delta\Delta Ct}$ method. The ct values of target genes were normalized to reference gene, ribosomal protein 49 (*rp49*).

Imaging of retinal pigment cell degeneration

Twenty- and thirty-day-old female adults were collected and their eye depigmentation phenotypes were recorded. At least 30 individuals for each genotype were examined under a microscope, and at least five representative individuals were chosen for imaging. Pictures were taken with an EOS 550D camera (Canon) mounted on a SteREO Discovery V8 microscope (Zeiss).

Immunostaining

Brains dissected from 10- or 20-day-old adult females were used for immunostaining. The brains were fixed in 4% PFA, permeabilized with PBST (0.1% Triton X-100), blocked in PAT (PBS, 0.1% Triton X-100, 1% BSA) and stained with antibodies in PBT (PBS, 0.3% Triton X-100, 0.1% BSA). Primary antibodies used in this study were mouse anti-HTT, MW8 which specifically binds to mHTT aggregates (1:40, DSHB), and rat anti-Elav (1:40, DSHB) which is a pan-neuronal antibody. Secondary antibodies were Alexa Fluor 488 anti-mouse and Alexa Fluor 647 anti-rat (1:200, Invitrogen). The samples were mounted in Fluoromount-G (Thermo Fisher) overnight, prior to image examination.

Quantification of mHTT aggregates

Images of aggregates were taken using a Flowview 100 confocal microscope (Olympus). The intensity of mHTT aggregates detected by anti-HTT antibody (MW8) or anti-Elav were quantified using ImageJ software. The level of mHTT aggregates was quantified by normalizing the mHTT aggregates intensity to Elav intensity. At least six brain images from each genotype were analyzed.

AMPK inhibitor (dorsomorphin) feeding

Thirty first instar of Q20- or Q93-exexpressing larvae were collected for each replicate 24 hours after egg laying. Larvae were transferred to fresh vials with 0.5 g instant *Drosophila* medium (Formula 4–24, Carolina Biological Supply, Burlington, NC) supplemented with 2 mL distilled water containing either dorsomorphin (100 μM) or DMSO (1%). Total number of emerging adults were counted.

Statistical analysis

Error bars show standard error of the mean throughout this paper. Significance was established using Student's t-test (N.S., not significant; * $P < 0.05$, ** $P < 0.01$, *** $P < 0.001$) or one-way ANOVA analysis with Tukey's HSD *post-hoc* test. For the statistical analysis of survival curves, we used the online tool OASIS 2 to perform a weighted log-rank test (Wilcoxon-Breslow-Gehan test) for determining significance[73].

473 **Figures**

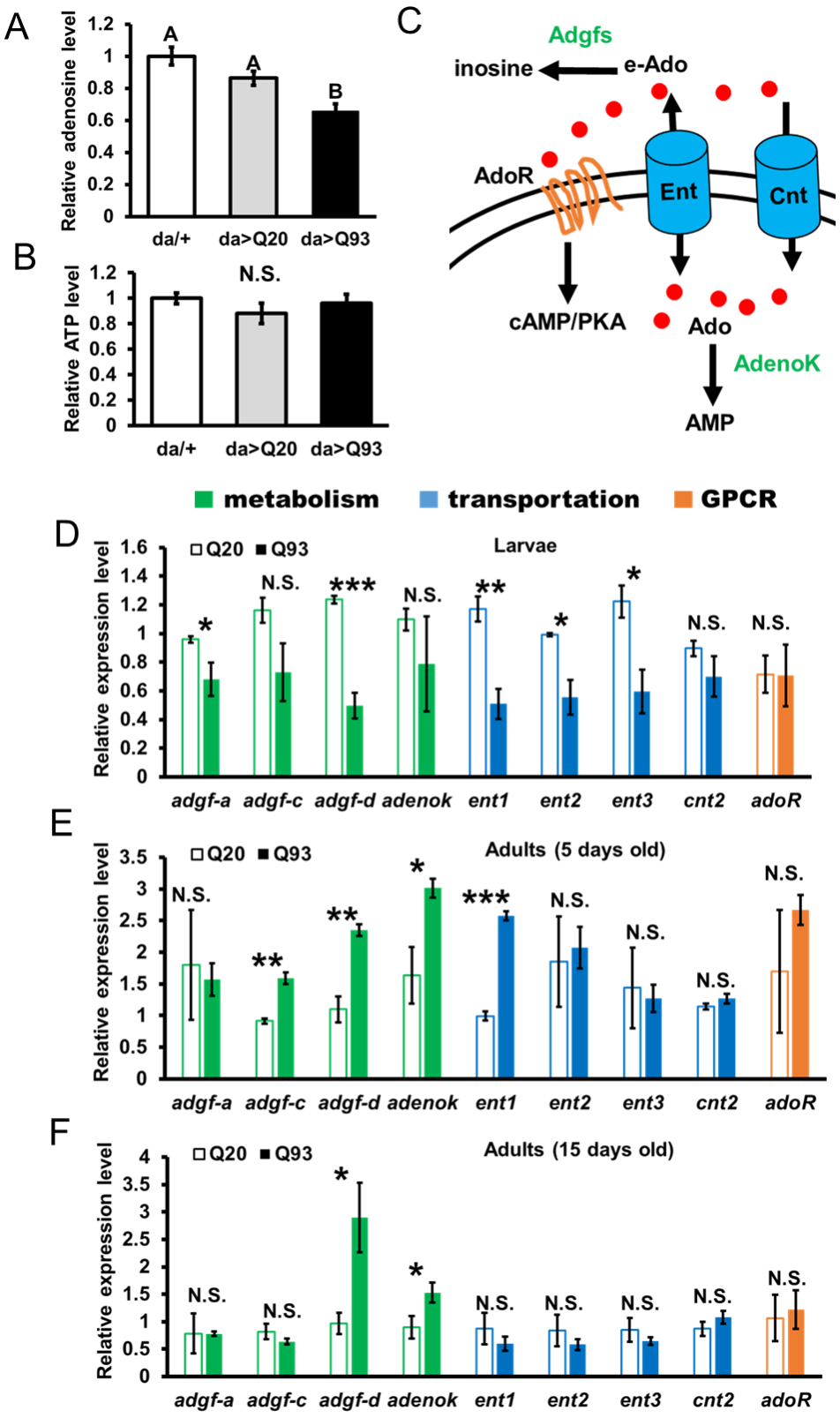

474

Figure 1. Alteration of adenosine homeostasis in the *Drosophila* HD model. (A-B) The measurements of extracellular adenosine levels (A) and extracellular ATP levels (B) in Q93-expressing (da>Q93), Q20-expressing (da>Q20) and control *da*-GAL4 (da/+) larvae. Six independent replicates were measured. Significance was analyzed by ANOVA with Tukey's HSD *post-hoc* test; significant differences ($P < 0.05$) among treatment groups are marked with different letters. (C) Diagram showing the interaction of adenosine metabolic enzymes, transporters, and receptors in *Drosophila*. (D-F) Expression profiles of genes involved in adenosine metabolism (green) and adenosine transportation (blue) as well as adenosine receptors (orange) at different stages in HD *Drosophila* brains (larvae) or heads (adults). The expression of Q20 and Q93 were driven by the pan-neuronal driver (*elav*-GAL4). Three independent replicates were measured. The significances of results were examined using Student's t-test: $*P < 0.05$, $**P < 0.01$, $***P < 0.001$; N.S., not significant. All data are presented as mean ± SEM

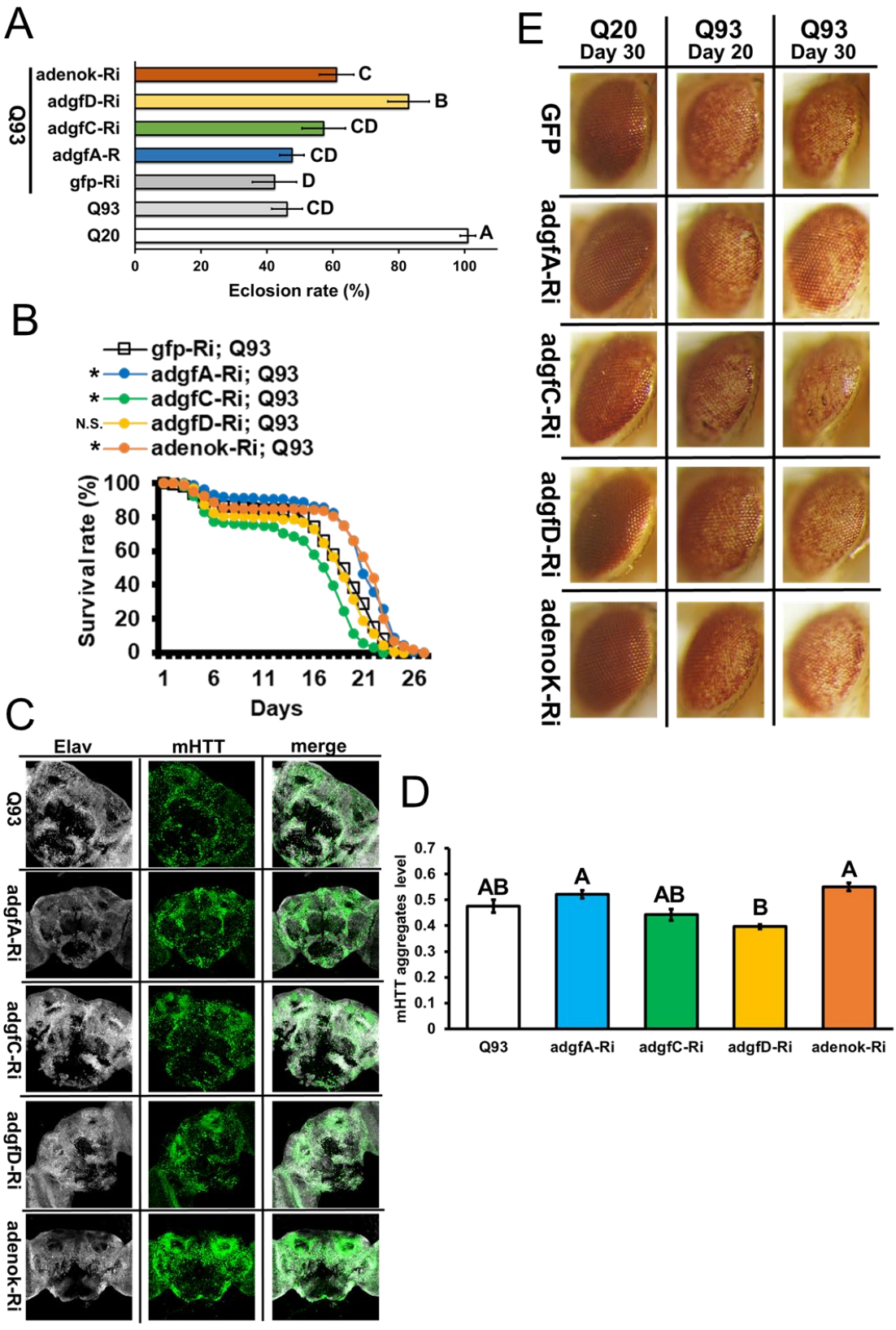

501

502

Figure 2. RNAi-mediated (Ri) downregulation of adenosine metabolic genes in HD *Drosophila*. Co-expression Q93 with each RNAi transgenes were driven by the pan-neuronal driver, *elav*-GAL4 (A-D), or eye driver, *gmr-GAL4* (E). The adult eclosion rate (A), adult lifespan (B), mHTT aggregate levels (C-D), and retinal pigment cell degeneration (E) were compared. † Eye image of homozygous *adoR*^{1} mutant without *htt* expression. At least five independent replicates were measured for eclosion rate. Detailed methodologies of the lifespan assay, eye imaging, and quantification of mHTT aggregates are described in Materials and methods. Significance values of the eclosion rate (A) and mHTT aggregates levels (D) were analyzed by ANOVA with Tukey's HSD *post-hoc* test; significant differences ($P < 0.05$) among treatment groups are marked with different letters. Significance values for the adult lifespan curve (B) were analyzed by a weighted log-rank test, and significant differences between control gfp-Ri flies with each RNAi group are labeled as follows: *$P < 0.05$; N.S., not significant. Error bars are presented as mean ± SEM

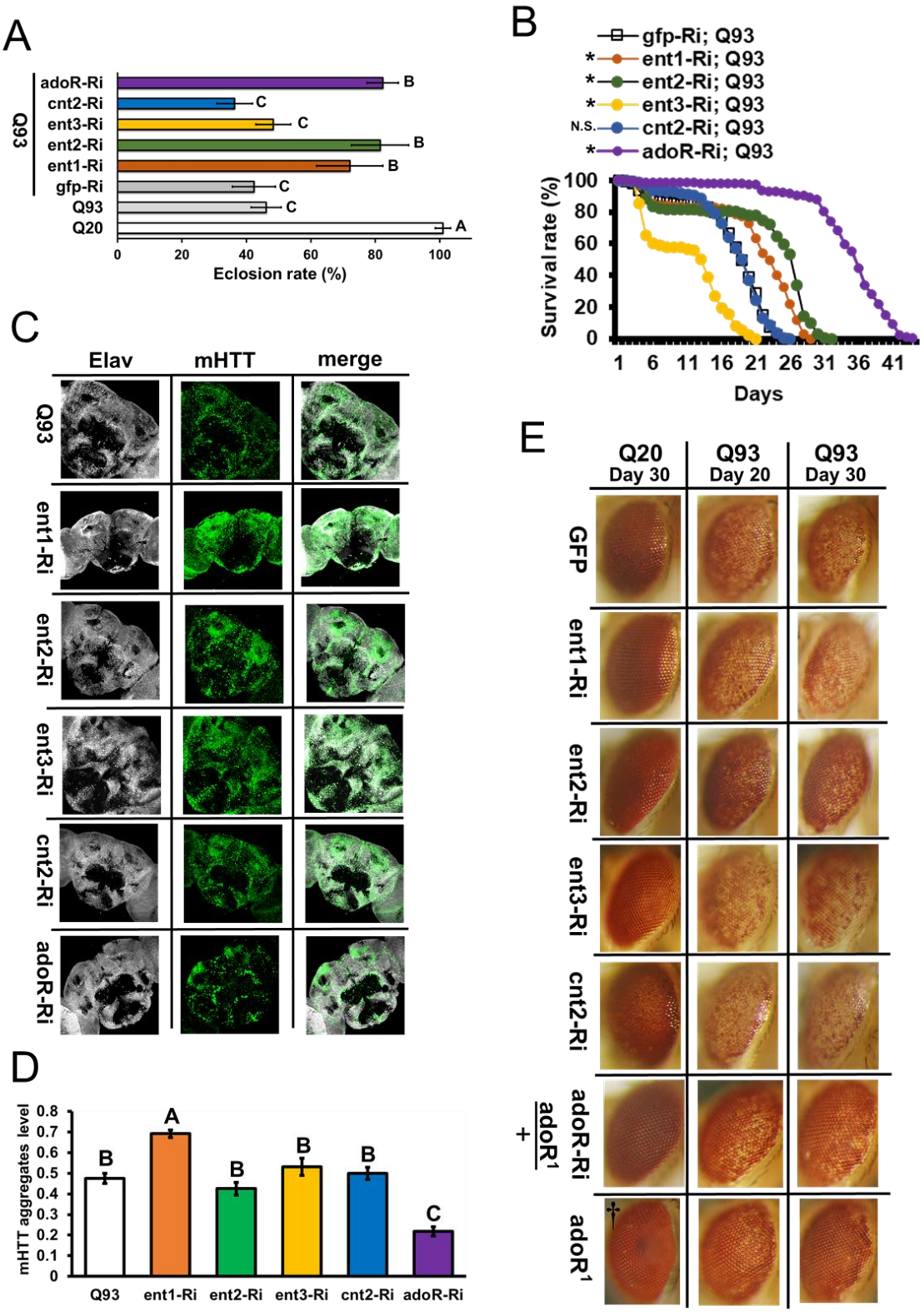

529

530

Figure 3. RNAi-mediated (Ri) downregulation of adenosine transporters and adenosine receptor (*adoR*) in HD *Drosophila*. Co-expression of Q93 with each RNAi transgene was driven by the pan-neuronal driver, *elav*-GAL4 (A-D), or eye driver, *gmr*-GAL4 (E). The adult eclosion rate (A), adult lifespan (B), mHTT aggregate levels (C-D), and retinal pigment cell degeneration (E) were compared. At least five independent replicates were measured for eclosion rate. Detailed methodologies of the lifespan assay, eye imaging, and quantification of mHTT aggregates are described in Materials and methods. Significance values for eclosion rate (A) and mHTT aggregates levels (D) were analyzed by ANOVA with Tukey's HSD *post-hoc* test; significant differences ($P < 0.05$) among treatment groups are marked with different letters. Significance values for the adult lifespan curve (B) were analyzed by a weighted log-rank test; significant differences comparing control gfp-Ri with each RNAi group are labeled as follows: $*P < 0.05$; N.S., not significant. Error bar are presented as mean ± SEM

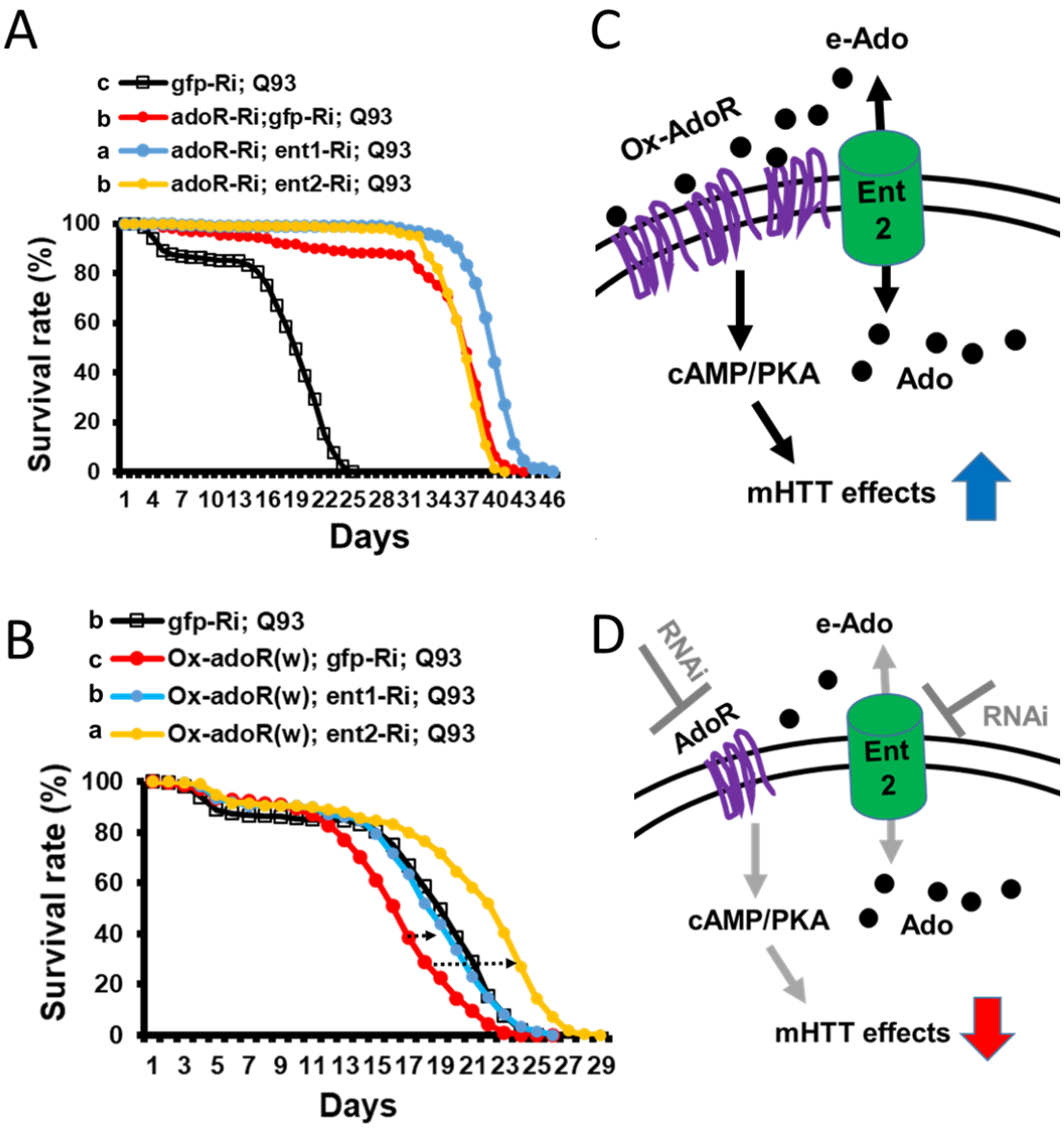

Figure 4. Interactions of AdoR and ENTs in HD *Drosophila*. (A) Co-expression of *adoR* RNAi with *ent1* or *ent2* RNAi in HD flies. (B) Co-expression of *adoR* overexpressing construct (Ox-adoR) with *ent1* or *ent2* RNAi transgenes in HD flies. Significance values of the adult lifespan curve were analyzed by a weighted log-rank test; different letters indicate significant differences ($P < 0.05$) among treatment groups. (C-D) Diagrams showing the action of Ado in mHTT pathogenesis

A

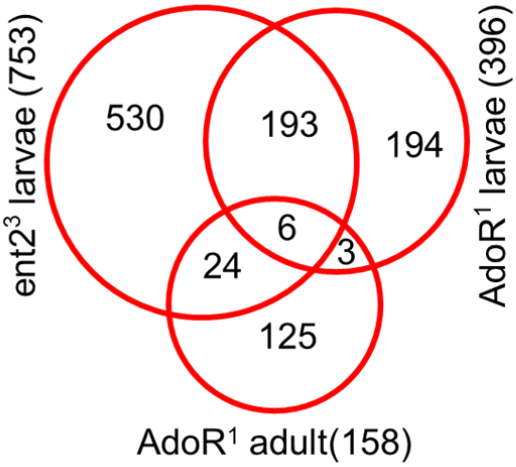

B

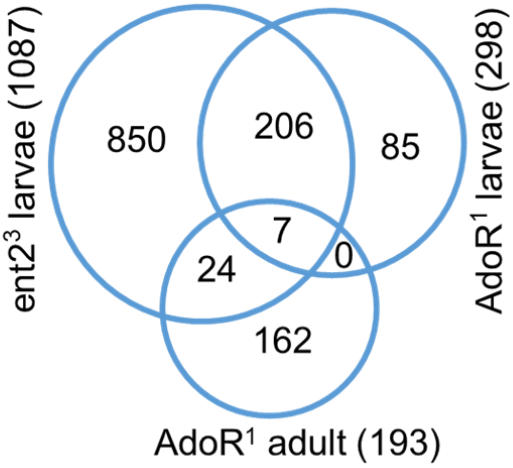

C

Probe ID	gene	CG	Log fold change			Localization
			Ent2³-L	AdoR¹-L	AdoR¹-A	
1641190_at	Jon65Aii	CG6580	2.79	2.5	3.18	MG
1627771_at		CG13075	2.58	2.91	1.93	HG, MT
1630590_at		CG18417	2.02	3.48	4.35	MG, HG
1624393_at	w	CG2759	1.77	4.97	4.5	MT
1632003_a_at	Ptp99A	CG11516	1.53	1.41	2.32	ID, NS, T
1632404_at	rtet	CG5760	1.02	0.85	2.09	MG, HG, I
1633369_s_at		CG6184	-0.23	-0.21	-0.68	NS, tes
1637389_at	Ir100a	CG11575	-0.67	-0.68	-2.61	non-spec
1635901_at		CG17197	-0.85	-0.63	-1.09	ID, tes
1624020_at	mod(mdg4)	CG32491	-1	-1.4	-0.57	NS, ID
1640850_at	cindr	CG31012	-1.11	-1.1	-1.02	NS, SS, ID, tes
1627953_at	mod(mdg4)	CG32491	-1.28	-1.08	-1.19	NS, ID
1633748_at	ND-20L	CG2014	-1.94	-2.05	-0.82	ID, tes

D

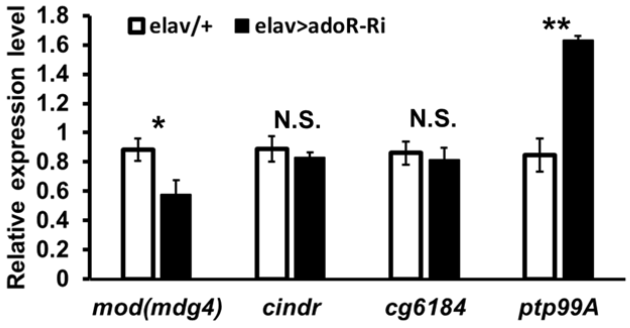

E

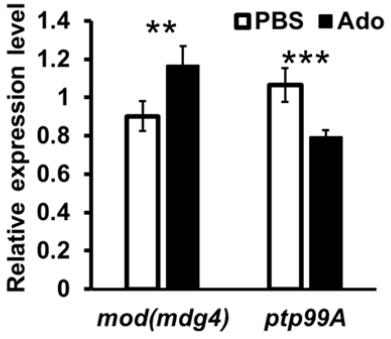

566

Figure 5. Identification of potential downstream targets of AdoR by microarray analysis. (A-B) Venn diagram showing the number of common genes (in intersect region) which are upregulated (A) or downregulated (B) among the *adoR* mutant larvae vs. control (w^{1118}), *adoR* mutant adults vs. control (w^{1118}), and *ent2* mutant larvae vs. control (w^{1118}). The cutoff values for expression differences were set at $Q < 0.05$ (false discovery rate, FDR). (C) The intersection between the three datasets; tissue localization of each gene expression was obtained from Flybase (http://flybase.org/). Tissue abbreviations: midgut (MG), hindgut (HG), Malpighian tubule (MT), imaginal disc (ID), integument (I), sensory system (SS), nervous system (NS), trachea (T), testis (tes), nonspecific expression (non-spec) (D) qPCR confirmed the potential AdoR-regulated genes expressed in the nervous system. Expression of *adoR* RNAi transgenes (adoR-Ri) was driven by the pan-neuronal driver (elav>adoR-Ri), and control flies contained *elav*-GAL4 (elav/+) only. (E) Enhancing extracellular adenosine signaling by adenosine injection and qPCR examination demonstrated that *mod(mdg4)* is positively- and *ptp99A* is negatively-regulated by adenosine signaling. Three independent replicates were measured in qPCR experiments. The qPCR primers of *mod(mdg4)* were selected to target the common 5′ exon shared in all of the isoforms. Student's t-test was used to examine the significance of qPCR results: $*P < 0.05$, $**P < 0.01$, $***P < 0.001$; N.S., not significant. Error bars are presented as averages ± SEM

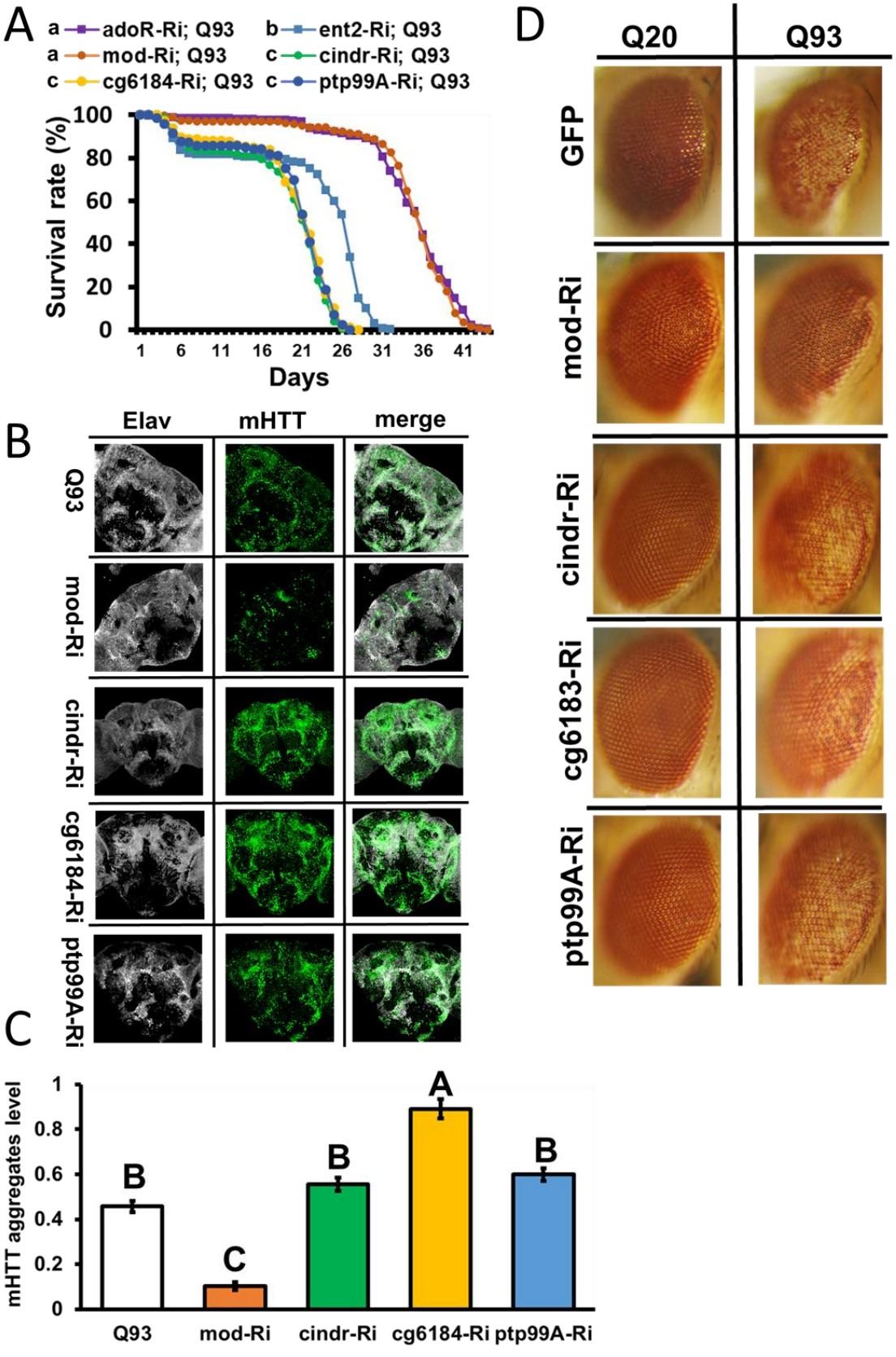

595

Figure 6. RNAi-mediated (Ri) downregulation of potential downstream targets of AdoR signaling in HD *Drosophila*. Co-expression of Q93 with each RNAi transgene, including *ptp99A*, *CG6184*, *cindr*, and *mod(mdg4)*, were driven by the pan-neuronal driver, *elav*-GAL4 (A-B), or the eye driver, *gmr*-GAL4 (D). The adult lifespan (A), mHTT aggregate levels (B-C), and retinal pigment cell degeneration (D) were compared. A detailed methodology of the lifespan assay, eye imaging, and quantification of mHTT aggregates are described in Materials and methods. Significance values of the adult lifespan curve (A) were analyzed by a weighted log-rank test, and different letters indicate significant differences ($P < 0.05$) among treatment groups. Significance values of mHTT aggregate levels (C) were analyzed by ANOVA with Tukey's HSD *post-hoc* test; significant differences ($P < 0.05$) among treatment groups are marked with different letters. Error bars are presented as mean ± SEM

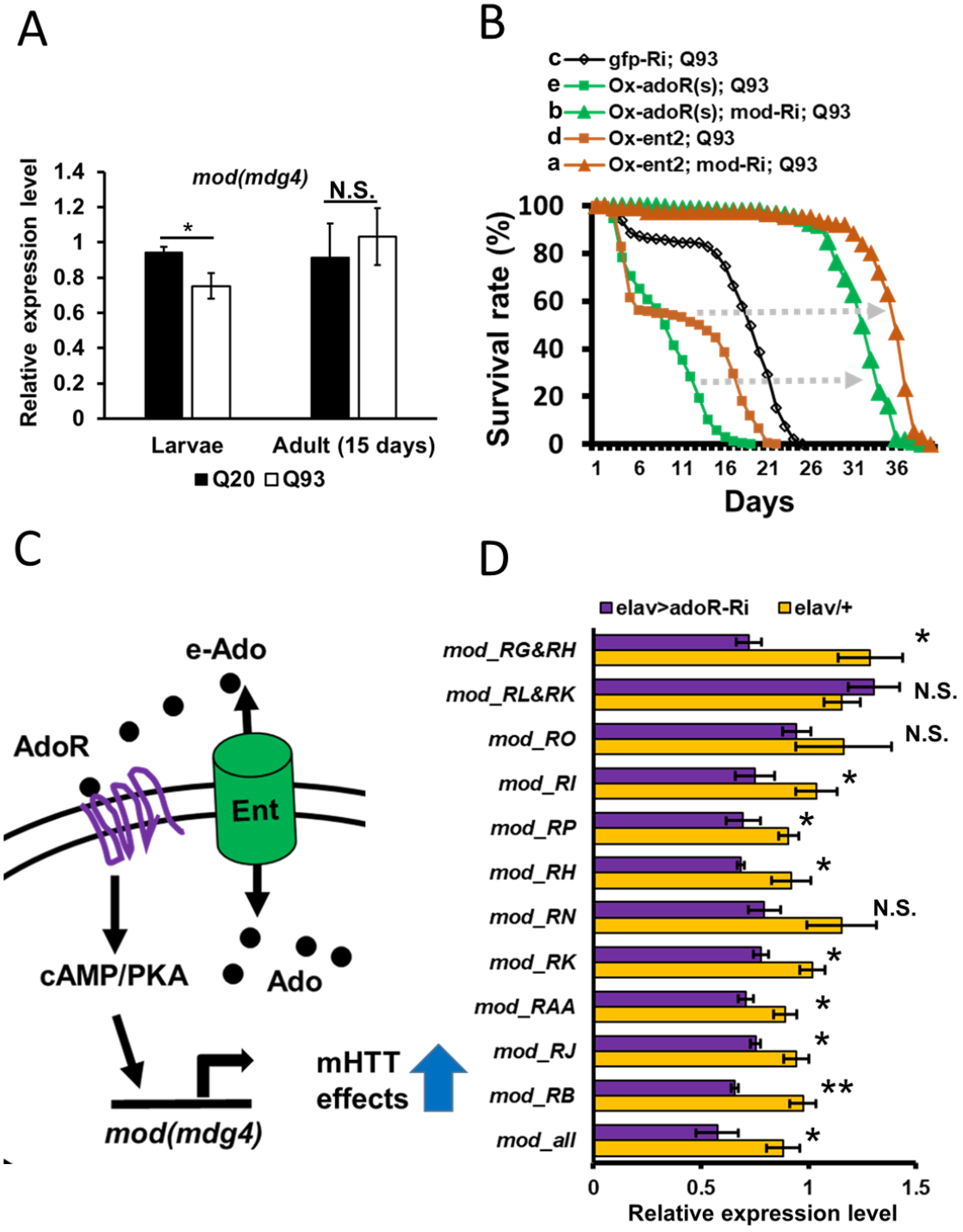

622

623

624

Figure 7. *mod(mdg4)* as a AdoR-regulated gene contributes to HD pathogenesis. (A) qPCR analysis of the expression of *mod(mdg4)* in the larval brain and 15-day-old adult heads of Q20- and Q93-expressing flies. The qPCR primers of *mod(mdg4)* targeted the common 5′ exon shared by all isoforms. (B) Epistasis analysis showed that *ent2* (Ox-ent2) and *adoR* overexpression (Ox-adoR) with *mod(mdg4)* RNAi transgenes in HD flies decreased the mortality effect caused by *ent2* and *adoR* overexpression. This suggests that *mod(mdg4)* is downstream of the AdoR pathway (C). qPCR identified potential *mod(mdg4)* isoforms regulated by the AdoR pathway. *adoR* RNAi transgene (adoR-Ri) expression was driven by the pan-neuronal driver (elav>adoR-Ri); control flies contained only *elav*-GAL*4* (elav/+). Mod_all indicates that the primers targeted all *mod(mdg4)* isoforms. Isoforms L and G do not have their own unique exonal region, therefore it is possible for the qPCR primers to target two isoforms simultaneously (presented as RG&RG and RL&RK). qPCR result significance was examined using Student's t-test: $*P < 0.05$, $**P < 0.01$, $***P < 0.001$; N.S., not significant. Significance values for the adult lifespan curve (A) were analyzed by weighted log-rank test, and different letters indicate significant differences ($P < 0.05$) among treatment groups. Error bars are presented as mean ± SEM

Acknowledgements

We thank Dr. Ingrid Poernbacher (The Francis Crick Institute, UK), Prof. Lawrence Marsh (UC Irvine, USA), Dr. Marek Jindra (Biology Centre CAS, Czechia), Dr. Tomas Dolezal (University of South Bohemia, Czechia), Dr. Ulrich Theopold (Stockholm University), Bloomington *Drosophila* Stock Center and Vienna *Drosophila* Resource Center for providing us with fly strains. This work was supported by the grant agency of the University of South Bohemia (065/2017/P to Y-HL), junior grant project GACR (19-13784Y to LK) and European Community's Programme Interreg Östereich-Tschechische Republik (REGGEN/ATCZ207 to MZ).

Author Contributions

Y-HL performed the experiments and prepared the manuscript. HM assisted in recording the adult lifespan and eye phenotypes as well as performed the brain dissection, immunochemistry and confocal microscopy imaging. LK performed the sample preparation and analyzed the microarray data. LR assisted in recording the adult lifespan, eye phenotype and prepared fly strains. TF established the methodologies for recording the eclosion rate, survival and prepared fly strains. MZ conceived the project and supervised manuscript preparation.

References

1 Dunwiddie, T. V. & Masino, S. A. The role and regulation of adenosine in the central nervous system. *Annu Rev Neurosci* **24**, 31-55, doi:10.1146/annurev.neuro.24.1.31 (2001).

2 Cunha, R. A. Adenosine as a neuromodulator and as a homeostatic regulator in the nervous system: different roles, different sources and different receptors. *Neurochemistry International* **38**, 107-125, doi:Doi 10.1016/S0197-0186(00)00034-6 (2001).

3 Fredholm, B. B. Adenosine, an endogenous distress signal, modulates tissue damage and repair. *Cell Death Differ* **14**, 1315-1323, doi:10.1038/sj.cdd.4402132 (2007).

4 Picano, E. & Abbracchio, M. P. Adenosine, the imperfect endogenous anti-ischemic cardio-neuroprotector. *Brain Res Bull* **52**, 75-82, doi:10.1016/s0361-9230(00)00249-5 (2000).

5 Xiao, C., Liu, N., Jacobson, K. A., Gavrilova, O. & Reitman, M. L. Physiology and effects of nucleosides in mice lacking all four adenosine receptors. *PLoS Biol* **17**, e3000161, doi:10.1371/journal.pbio.3000161 (2019).

6 Cunha, R. A. Signaling by adenosine receptors-Homeostatic or allostatic control? *PLoS Biol* **17**, e3000213, doi:10.1371/journal.pbio.3000213 (2019).

7 Lee, C. F. & Chern, Y. J. Adenosine Receptors and Huntington's Disease. *Int Rev Neurobiol* **119**, 195-232, doi:10.1016/B978-0-12-801022-8.00010-6 (2014).

8 Vonsattel, J. P. & DiFiglia, M. Huntington disease. *J Neuropathol Exp Neurol* **57**, 369-384, doi:10.1097/00005072-199805000-00001 (1998).

9 Blum, D., Hourez, R., Galas, M.-C., Popoli, P. & Schiffmann, S. N. Adenosine receptors and Huntington's disease: implications for pathogenesis and therapeutics. *The Lancet Neurology* **2**, 366-374, doi:https://doi.org/10.1016/S1474-4422(03)00411-3 (2003).

10 Blum, D. *et al.* in *The Adenosine Receptors* (eds Pier Andrea Borea *et al.*) 281-308 (Springer International Publishing, 2018).

11 Gomes, C. V., Kaster, M. P., Tome, A. R., Agostinho, P. M. & Cunha, R. A. Adenosine receptors and brain diseases: Neuroprotection and neurodegeneration. *Bba-Biomembranes* **1808**, 1380-1399, doi:10.1016/j.bbamem.2010.12.001 (2011).

12 Kao, Y. H. *et al.* Targeting ENT1 and adenosine tone for the treatment of Huntington's disease. *Hum Mol Genet* **26**, 467-478, doi:10.1093/hmg/ddw402 (2017).

13 Guitart, X. *et al.* Equilibrative nucleoside transporter ENT1 as a biomarker of Huntington disease. *Neurobiol Dis* **96**, 47-53, doi:10.1016/j.nbd.2016.08.013 (2016).

14 Tyebji, S. *et al.* Hyperactivation of D1 and A2A receptors contributes to cognitive dysfunction in Huntington's disease. *Neurobiol Dis* **74**, 41-57, doi:10.1016/j.nbd.2014.11.004 (2015).

15 Anderson, C. M. & Nedergaard, M. Emerging challenges of assigning P2X7 receptor function and immunoreactivity in neurons. *Trends Neurosci* **29**, 257-262, doi:10.1016/j.tins.2006.03.003 (2006).

16 Lewis, E. A. & Smith, G. A. Using Drosophila models of Huntington's disease as a translatable tool. *J Neurosci Methods* **265**, 89-98, doi:10.1016/j.jneumeth.2015.07.026 (2016).

17 Steffan, J. S. *et al.* Histone deacetylase inhibitors arrest polyglutamine-dependent neurodegeneration in Drosophila. *Nature* **413**, 739-743, doi:Doi 10.1038/35099568 (2001).

18 Kucerova, L. *et al.* Characterization of the Drosophila adenosine receptor: the effect of adenosine analogs on cAMP signaling in Drosophila cells and their utility for in vivo experiments. *J Neurochem* **121**, 383-395, doi:10.1111/j.1471-4159.2012.07701.x (2012).

19 Fountain, S. J. Primitive ATP-activated P2X receptors: discovery, function and pharmacology. *Front Cell Neurosci* **7**, 247, doi:10.3389/fncel.2013.00247 (2013).

20 Maier, S. A., Galellis, J. R. & McDermid, H. E. Phylogenetic analysis reveals a novel protein family closely related to adenosine deaminase. *J Mol Evol* **61**, 776-794, doi:10.1007/s00239-005-0046-y (2005).

21 Zurovec, M., Dolezal, T., Gazi, M., Pavlova, E. & Bryant, P. J. Adenosine deaminase-related growth factors stimulate cell proliferation in Drosophila by depleting extracellular adenosine. *Proc Natl Acad Sci U S A* **99**, 4403-4408, doi:10.1073/pnas.062059699 (2002).

22 Stenesen, D. *et al.* Adenosine nucleotide biosynthesis and AMPK regulate adult life span and mediate the longevity benefit of caloric restriction in flies. *Cell Metab* **17**, 101-112, doi:10.1016/j.cmet.2012.12.006 (2013).

23 Bajgar, A. *et al.* Extracellular adenosine mediates a systemic metabolic switch during immune response. *PLoS Biol* **13**, e1002135, doi:10.1371/journal.pbio.1002135 (2015).

24 Poernbacher, I. & Vincent, J. P. Epithelial cells release adenosine to promote local TNF production in response to polarity disruption. *Nat Commun* **9**, 4675, doi:10.1038/s41467-018-07114-z (2018).

25 Knight, D. *et al.* Equilibrative nucleoside transporter 2 regulates associative learning and synaptic function in Drosophila. *J Neurosci* **30**, 5047-5057, doi:10.1523/JNEUROSCI.6241-09.2010 (2010).

26 Song, W. *et al.* Morphometric analysis of Huntington's disease neurodegeneration in Drosophila. *Methods in molecular biology (Clifton, N.J.)* **1017**, 41-57, doi:10.1007/978-1-62703-438-8_3 (2013).

27 Kao, Y. H. *et al.* Targeting ENT1 and adenosine tone for the treatment of Huntington's disease. *Human Molecular Genetics* **26**, 467-478, doi:10.1093/hmg/ddw402 (2017).

28 Martinez-Mir, M. I., Probst, A. & Palacios, J. M. Adenosine-A2 Receptors - Selective Localization in the Human Basal Ganglia and Alterations with Disease. *Neuroscience* **42**, 697-706, doi:Doi 10.1016/0306-4522(91)90038-P (1991).

29 Glass, M., Dragunow, M. & Faull, R. L. M. The pattern of neurodegeneration in Huntington's disease: A comparative study of cannabinoid, dopamine, adenosine and GABA(A) receptor alterations in the human basal ganglia in Huntington's disease. *Neuroscience* **97**, 505-519, doi:Doi 10.1016/S0306-4522(00)00008-7 (2000).

30 Mievis, S., Blum, D. & Ledent, C. A2A receptor knockout worsens survival and motor behaviour in a transgenic mouse model of Huntington's disease. *Neurobiol Dis* **41**, 570-576, doi:10.1016/j.nbd.2010.09.021 (2011).

31 Bajgar, A. & Dolezal, T. Extracellular adenosine modulates host-pathogen interactions through regulation of systemic metabolism during immune response in Drosophila. *PLoS Pathog* **14**, e1007022, doi:10.1371/journal.ppat.1007022 (2018).

32 Zuberova, M., Fenckova, M., Simek, P., Janeckova, L. & Dolezal, T. Increased extracellular adenosine in Drosophila that are deficient in adenosine deaminase activates a release of energy stores leading to wasting and death. *Dis Model Mech* **3**, 773-784, doi:10.1242/dmm.005389 (2010).

33 Kuo, Y., Ren, S., Lao, U., Edgar, B. A. & Wang, T. Suppression of polyglutamine protein toxicity by co-expression of a heat-shock protein 40 and a heat-shock protein 110. *Cell Death Dis* **4**, e833, doi:10.1038/cddis.2013.351 (2013).

34 Mugat, B., Parmentier, M. L., Bonneaud, N., Chan, H. Y. & Maschat, F. Protective role of Engrailed in a Drosophila model of Huntington's disease. *Hum Mol Genet* **17**, 3601-3616, doi:10.1093/hmg/ddn255 (2008).

35 Aymerich, I., Foufelle, F., Ferre, P., Casado, F. J. & Pastor-Anglada, M. Extracellular adenosine activates AMP-dependent protein kinase (AMPK). *J Cell Sci* **119**, 1612-1621, doi:10.1242/jcs.02865 (2006).

36 Dolinar, K., Jan, V., Pavlin, M., Chibalin, A. V. & Pirkmajer, S. Nucleosides block AICAR-stimulated activation of AMPK in skeletal muscle and cancer cells. *Am J Physiol Cell Physiol* **315**, C803-C817, doi:10.1152/ajpcell.00311.2017 (2018).

37 Medina-Pulido, L. *et al.* Hypoxia and P1 receptor activation regulate the high-affinity concentrative adenosine transporter CNT2 in differentiated neuronal PC12 cells. *Biochem J* **454**, 437-445, doi:10.1042/BJ20130231 (2013).

38 Liu, H. *et al.* Elevated ecto-5'-nucleotidase: a missing pathogenic factor and new therapeutic target for sickle cell disease. *Blood Adv* **2**, 1957-1968, doi:10.1182/bloodadvances.2018015784 (2018).

39 Ruan, C. C. *et al.* A(2A) Receptor Activation Attenuates Hypertensive Cardiac Remodeling via Promoting Brown Adipose Tissue-Derived FGF21. *Cell Metabolism* **28**, 476-+, doi:10.1016/j.cmet.2018.06.013 (2018).

40 Vazquez-Manrique, R. P. *et al.* AMPK activation protects from neuronal dysfunction and vulnerability across nematode, cellular and mouse models of Huntington's disease. *Hum Mol Genet* **25**, 1043-1058, doi:10.1093/hmg/ddv513 (2016).

41 Ju, T. C. *et al.* Nuclear translocation of AMPK-alpha1 potentiates striatal neurodegeneration in Huntington's disease. *J Cell Biol* **194**, 209-227, doi:10.1083/jcb.201105010 (2011).

42 Swick, L. L., Kazgan, N., Onyenwoke, R. U. & Brenman, J. E. Isolation of AMP-activated protein kinase (AMPK) alleles required for neuronal maintenance in Drosophila melanogaster. *Biol Open* **2**, 1321-1323, doi:10.1242/bio.20136775 (2013).

43 Johnson, E. C. *et al.* Altered metabolism and persistent starvation behaviors caused by reduced AMPK function in Drosophila. *PLoS One* **5**, doi:10.1371/journal.pone.0012799 (2010).

44 Braco, J. T., Gillespie, E. L., Alberto, G. E., Brenman, J. E. & Johnson, E. C. Energy-dependent modulation of glucagon-like signaling in Drosophila via the AMP-activated protein kinase. *Genetics* **192**, 457-466, doi:10.1534/genetics.112.143610 (2012).

45 Yu, S., Waldholm, J., Bohm, S. & Visa, N. Brahma regulates a specific trans-splicing event at the mod(mdg4) locus of Drosophila melanogaster. *RNA Biol* **11**, 134-145, doi:10.4161/rna.27866 (2014).

46 Blum, D. *et al.* The Role of Adenosine Tone and Adenosine Receptors in Huntington's Disease. *J Caffeine Adenosine Res* **8**, 43-58, doi:10.1089/caff.2018.0006 (2018).

47 Gianfriddo, M., Melani, A., Turchi, D., Giovannini, M. G. & Pedata, F. Adenosine and glutamate extracellular concentrations and mitogen-activated protein kinases in the striatum of Huntington transgenic mice. Selective antagonism of adenosine A2A receptors reduces transmitter outflow. *Neurobiol Dis* **17**, 77-88, doi:10.1016/j.nbd.2004.05.008 (2004).

48 Domenici, M. R. *et al.* Behavioral and electrophysiological effects of the adenosine A2A receptor antagonist SCH 58261 in R6/2 Huntington's disease mice. *Neurobiol Dis* **28**, 197-205, doi:10.1016/j.nbd.2007.07.009 (2007).

49 Blum, D., Hourez, R., Galas, M. C., Popoli, P. & Schiffmann, S. N. Adenosine receptors and Huntington's disease: implications for pathogenesis and therapeutics. *Lancet Neurol* **2**, 366-374, doi:10.1016/s1474-4422(03)00411-3 (2003).

50 Fleischmannova, J. *et al.* Differential response of Drosophila cell lines to extracellular adenosine. *Insect Biochem Mol Biol* **42**, 321-331, doi:10.1016/j.ibmb.2012.01.002 (2012).

51 Toczek, M. *et al.* An impaired metabolism of nucleotides underpins a novel mechanism of cardiac remodeling leading to Huntington's disease related cardiomyopathy. *Biochim Biophys Acta* **1862**, 2147-2157, doi:10.1016/j.bbadis.2016.08.019 (2016).

52 Dorn, R. & Krauss, V. The modifier of mdg4 locus in Drosophila: functional complexity is resolved by trans splicing. *Genetica* **117**, 165-177, doi:Doi 10.1023/A:1022983810016 (2003).

53 Mutsuddi, M., Marshall, C. M., Benzow, K. A., Koob, M. D. & Rebay, I. The spinocerebellar ataxia 8 noncoding RNA causes neurodegeneration and associates with staufen in Drosophila. *Curr Biol* **14**, 302-308, doi:10.1016/j.cub.2004.01.034 (2004).

54 van Eyk, C. L. *et al.* Perturbation of the Akt/Gsk3-beta signalling pathway is common to Drosophila expressing expanded untranslated CAG, CUG and AUUCU repeat RNAs. *Hum Mol Genet* **20**, 2783-2794, doi:10.1093/hmg/ddr177 (2011).

55 Krauss, V. & Dorn, R. Evolution of the trans-splicing Drosophila locus mod(mdg4) in several species of Diptera and Lepidoptera. *Gene* **331**, 165-176, doi:10.1016/j.gene.2004.02.019 (2004).

56 Bardwell, V. J. & Treisman, R. The POZ domain: a conserved protein-protein interaction motif. *Genes Dev* **8**, 1664-1677, doi:10.1101/gad.8.14.1664 (1994).

57 Espinas, M. L. *et al.* The N-terminal POZ domain of GAGA mediates the formation of oligomers that bind DNA with high affinity and specificity. *J Biol Chem* **274**, 16461-16469, doi:10.1074/jbc.274.23.16461 (1999).

58 Albagli, O., Dhordain, P., Deweindt, C., Lecocq, G. & Leprince, D. The BTB/POZ domain: a new protein-protein interaction motif common to DNA- and actin-binding proteins. *Cell Growth Differ* **6**, 1193-1198 (1995).

59 Thomas, S. E. *et al.* Identification of two proteins required for conjunction and regular segregation of achiasmate homologs in Drosophila male meiosis. *Cell* **123**, 555-568, doi:10.1016/j.cell.2005.08.043 (2005).

60 Soltani-Bejnood, M. *et al.* Role of the mod(mdg4) common region in homolog segregation in Drosophila male meiosis. *Genetics* **176**, 161-180, doi:10.1534/genetics.106.063289 (2007).

61 Buchner, K. *et al.* Genetic and molecular complexity of the position effect variegation modifier mod(mdg4) in Drosophila. *Genetics* **155**, 141-157 (2000).

62 Soshnev, A. A., Baxley, R. M., Manak, J. R., Tan, K. & Geyer, P. K. The insulator protein Suppressor of Hairy-wing is an essential transcriptional repressor in the Drosophila ovary. *Development* **140**, 3613-3623, doi:10.1242/dev.094953 (2013).

63 Melnikova, L., Kostyuchenko, M., Parshikov, A., Georgiev, P. & Golovnin, A. Role of Su(Hw) zinc finger 10 and interaction with CP190 and Mod(mdg4) proteins in recruiting the Su(Hw) complex to chromatin sites in Drosophila. *PLoS One* **13**, e0193497, doi:10.1371/journal.pone.0193497 (2018).

64 Giot, L. *et al.* A protein interaction map of Drosophila melanogaster. *Science* **302**, 1727-1736, doi:10.1126/science.1090289 (2003).

65 Oughtred, R. *et al.* The BioGRID interaction database: 2019 update. *Nucleic Acids Res* **47**, D529-D541, doi:10.1093/nar/gky1079 (2019).

66 Warrick, J. M. *et al.* Suppression of polyglutamine-mediated neurodegeneration in Drosophila by the molecular chaperone HSP70. *Nat Genet* **23**, 425-428, doi:10.1038/70532 (1999).

67 Chan, H. Y., Warrick, J. M., Gray-Board, G. L., Paulson, H. L. & Bonini, N. M. Mechanisms of chaperone suppression of polyglutamine disease: selectivity, synergy and modulation of protein solubility in Drosophila. *Hum Mol Genet* **9**, 2811-2820, doi:10.1093/hmg/9.19.2811 (2000).

68 Dolezal, T., Dolezelova, E., Zurovec, M. & Bryant, P. J. A role for adenosine deaminase in Drosophila larval development. *PLoS Biol* **3**, e201, doi:10.1371/journal.pbio.0030201 (2005).

69 Dolezelova, E., Nothacker, H. P., Civelli, O., Bryant, P. J. & Zurovec, M. A Drosophila adenosine receptor activates cAMP and calcium signaling. *Insect Biochem Mol Biol* **37**, 318-329, doi:10.1016/j.ibmb.2006.12.003 (2007).

70 Dolezal, T., Gazi, M., Zurovec, M. & Bryant, P. J. Genetic analysis of the ADGF multigene family by homologous recombination and gene conversion in Drosophila. *Genetics* **165**, 653-666 (2003).

71 Arefin, B. *et al.* Genome-wide transcriptional analysis of Drosophila larvae infected by entomopathogenic nematodes shows involvement of complement, recognition and extracellular matrix proteins. *J Innate Immun* **6**, 192-204, doi:10.1159/000353734 (2014).

72 Kucerova, L. *et al.* The Drosophila Chitinase-Like Protein IDGF3 Is Involved in Protection against Nematodes and in Wound Healing. *J Innate Immun* **8**, 199-210, doi:10.1159/000442351 (2016).

73 Han, S. K. *et al.* OASIS 2: online application for survival analysis 2 with features for the analysis of maximal lifespan and healthspan in aging research. *Oncotarget* **7**, 56147-56152, doi:10.18632/oncotarget.11269 (2016).